https://doi.org/10.48048/tis.2024.7788

Study of Ni-Co-ZrO_2/Al_2O_3 Catalysts for Carbon Dioxide Reforming of Methane at Low CO_2

Tanakorn Ratana[1,2], Lucksamon Thongdee[1], Sittichart Sawansombut[1], Wassachol Sumarasingha[1], Threeraphat Chutimaskul[3] and Monrudee Phongaksorn[1,2,*]

[1]Department of Industrial Chemistry, Faculty of Applied Science, King Mongkut's University of Technology North Bangkok, Bangkok 10800, Thailand
[2]Research and Development Center for Chemical Engineering Unit Operation and Catalyst Design (RCC), King Mongkut's University of Technology North Bangkok, Bangkok 10800, Thailand
[3]Nuclear Technology Research and Development Center, Thailand Institute of Nuclear Technology (Public Organisation), Nakorn Nayok 26120, Thailand

([*]Corresponding author's e-mail: monrudee.p@sci.kmutnb.ac.th)

Received: 30 November 2023, Revised: 28 December 2023, Accepted: 4 January 2024, Published: 10 May 2024

Abstract

This work studied the composition of Ni-Co-ZrO_2/Al_2O_3 catalyst on properties and efficiency of catalysts for carbon dioxide reforming of methane (CMR) when CO_2 was fed as the limiting reagent and CH_4 as the excess reactant. 9wt%Ni-1wt%ZrO_2/Al_2O_3, 4.5wt%Ni-4.5%wtCo-1wt%ZrO_2/Al_2O_3, 9wt%Co-1wt%ZrO_2/Al_2O_3 and 7wt%Co-3wt%ZrO_2/Al_2O_3 catalysts were prepared by wet impregnation method. The physicochemical properties of present catalysts were characterized by XRD, N_2 adsorption-desorption H_2-TPR and CO_2-TPD. The CRM performance was determined in a tubular fixed-bed reactor at 600 °C for 6 h with limiting of carbon dioxide. The carbon deposition on spent catalysts were examined by TGA. The results showed that Co-ZrO_2 catalysts provided greater activities, selectivity toward H_2 and stability than Ni-ZrO_2 and Ni-Co-ZrO_2 catalysts. 9wt%Co-1wt%ZrO_2/Al_2O_3 provided higher reactant conversions and H_2/CO ratio than 7wt%Co-3wt%ZrO_2/Al_2O_3 while the minimum coke formation was observed on spent 7wt%Co-3wt%ZrO_2/Al_2O_3. It is because oxophilic properties and oxygen vacancy sites in Co-ZrO_2 increase CO_2 dissociative adsorption as well as oxygen transport on the catalyst surface.

Keywords: CO_2 reforming of methane, Ni-Co catalyst, Co-based catalyst, Ni-Co-ZrO_2 catalyst Impregnation method, ZrO_2 promoter, Coke resistance

Introduction

At present, global warming is a major global crisis that causes severe climate variability. The main cause of global warming is the accumulation of greenhouse gases in the atmosphere. Carbon dioxide (CO_2) is the largest contributor while the second is methane (CH_4) that could trap heat 28 - 36 times more than carbon dioxide [1,2]. The key control of this issue is the reduction of carbon dioxide and methane emissions. To premise the key control of climate change, converting methane and carbon dioxide into alternative fuels and the intermediate raw material for high value chemical production is considered as a sustainable solution [3-5]. Among the industrial processes, carbon dioxide reforming of methane (CRM)) can be transformed to the mixture of hydrogen and carbon monoxide (syngas) written as Eq. (1). For products derived from CRM process, H_2 is a green fuel and syngas is a feedstock for both Fischer-Tropsch (FT) synthesis and chemical productions [6,7].

Ni-based catalysts are commonly used for CRM process in the case where the quantity of methane is equal to or less than carbon dioxide. The development of Ni-based catalysts has been mostly pointed toward the suppression of carbon deposition due to side reactions, the Boudouard reaction (Eq. (2)) and the methane cracking (Eq. (3)) [8]. When the carbon dioxide is excess, H_2 selectivity of catalysts decreases due to the reverse water gas shift side reaction (Eq. (4)) [9]. Many modification methods were applied to Ni-based catalysts to improve their CRM performance. The addition of alkaline and alkaline earth metal promoters or metal oxide promoters (K, Mg, etc.) increasing the basicity of catalyst [10,11] that can prevent methane cracking. Perovskite materials have been utilized as promoters or co-active species. CeO_2 can prevent the $NiAl_2O_4$ formation by forming $CeAlO_3$ and $Ce_{1-X}Ni_XO_2$, when Ce^{4+} reduced to Ce^{3+} ($CeO_2 \rightarrow CeO_{2-x}$), resulting in more the Ni active sites on the Ni/Al_2O_3 catalyst surface [12,13]. ZrO_2, as a promoter, enhanced

the dispersion of Ni metal on the catalyst [7]. CeO_2 and ZrO_2 provided the oxygen vacancy and oxygen storage properties that promoted H_2O activation-dissociation [6,7]. Co, another transition metals, was also added as a co-active metal. It was found that the oxophilic property of Co improved the dissociative adsorption of CO_2 during the reaction resulting in more oxygen mobility for carbon oxidation [14,15]. However, Co-based catalysts were tested in similar conditions, but they showed less performance toward CRM reaction than Ni-based catalysts [16].

$$CH_4\,(g) + CO_2\,(g) \rightarrow 2H_2\,(g) + 2CO\,(g) \qquad \Delta H°_{298} = +247\ \text{kJ/mol} \qquad (1)$$

$$2CO\,(g) \rightarrow C\,(s) + CO_2\,(g) \qquad \Delta H°_{298} = -173\ \text{kJ/mol} \qquad (2)$$

$$CH_4\,(g) \rightarrow C\,(s) + 2H_2\,(g) \qquad \Delta H°_{298} = +75\ \text{kJ/mol} \qquad (3)$$

$$CO_2\,(g) + H_2\,(g) \rightarrow CO\,(g) + H_2O\,(g) \qquad \Delta H°_{298} = +41\ \text{kJ/mol} \qquad (4)$$

Concerning the heat trapping ability of greenhouse gases, reducing methane emission in the atmosphere has much more effective impact than reducing carbon dioxide emission. To utilize CH_4 up to maximum quantity, CRM in the case that CO_2 is fed as the limiting reagent is considered and it is more challenging because this reaction condition can produce large amounts of coke. So, most studies avoid using this condition [6,7,10,12,15]. Moreover, the development of catalysts for CRM with high CH_4 concentration is more practical for petroleum industry. Thus, this work aims to develop Ni-Co-ZrO_2/Al_2O_3 catalysts and to evaluate the practical catalysts for CRM process with CO_2 is the limiting reagent. Four catalysts; 9wt%Co-1wt%ZrO_2/Al_2O_3, 7wt%Co-3wt%ZrO_2/Al_2O_3, 9wt%Ni-1wt%ZrO_2/Al_2O_3 and 4.5%wtNi-4.5%wtCo-1%wtZrO_2/Al_2O_3, prepared by incipient wetness impregnation were tested for CRM reaction in an in-house fixed-bed reactor. The anti-coking ability was evaluated using TGA analyzer. The conversion of reactants, selectivity and coke resistance were revealed and discussed corelating to their properties characterized by XRD, N_2 physisorption, H_2-TPR and CO_2-TPD.

Materials and methods

Materials

All precursors were obtained from the commercial suppliers and used in the synthesis of catalyst. Aluminium oxide (Al_2O_3, 98 %), Zirconium (IV) oxynitrate hydrate ($ZrO(NO_3)_2{\cdot}H_2O$, 98 %) and Cobalt (II) nitrate hexahydrate ($Co(NO_3)_2{\cdot}6H_2O$, 98 %) were purchased from Sigma Aldrich company. Nickel (II) nitrate hexahydrate ($Ni(NO_3)_2{\cdot}6H_2O$, 98 %) was purchased from Acros OrganicsTM company. All solutions were prepared with de-ionized water.

Catalysts preparation

The *x* wt.% Co-*y* wt.% ZrO_2/Al_2O_3 catalysts (denoted as *x*Co-*y*ZrO_2/Al_2O_3; *x:y* = 9:1 and 7:3) were prepared by wetness co-impregnation method. Before impregnation, the Al_2O_3 support was calcined in air at 650 °C for 5 h. The mixed solution of the desired amount of the cobalt nitrate solution and zirconium oxynitrate solution was added dropwise to Al_2O_3 support. The resulting wet powder was dried overnight at 60 °C and calcined in the air at 650 °C for 5 h with a heating rate of 5 °C min^{-1}.

Similarly, 9wt.%Ni-1wt.%ZrO_2/Al_2O_3 and 4.5wt.%Ni-4.5wt.%Co-1wt.%ZrO_2/Al_2O_3 catalyst (denoted as 9Ni-1ZrO_2/Al_2O_3 and 4.5Ni-4.5Co-1ZrO_2/Al_2O_3) were prepared by wetness co-impregnation method. The appropriate amount of the mixture of nickel nitrate solution, cobalt nitrate solution and zirconium oxynitrate solution was dropped onto the Al_2O_3 support. After impregnation, the powder product was dried and calcined using the similar conditions as those catalysts described above. All catalysts were pelletized, ground, and sieved to particle size range between 355 - 710 μm.

Catalysts characterization

The powder XRD patterns were recorded on a Rigaku SmartLab X-ray diffractometer (Rigaku, Tokyo, Japan) with Cu Kα λ = 0.154 nm, operating at 40 kV and 40 mA, and scanning with 2-theta between 10 to 80 ° using a step size of 0.01 °.

The surface properties and the pore structure were characterized by N_2 adsorption/desorption isotherm, which were measured at −196 °C of liquid nitrogen using BELSORP-mini II instrument (Osaka, Japan). Prior to the analysis, the degassing of all sample was performed at 350 °C under N_2 flow for 4 h to eliminate contaminated and moisture on the surface. Pore size distribution was calculated based on the

Barett-Joyner-Halenda (BJH) method. The specific surface area and pore volume were evaluated by the multipoint Brunauer-Emmett-Teller (BET) method.

The reducibility of the calcined catalyst was investigated through temperature programmed reduction of hydrogen (H_2-TPR) employing a BELCAT-basic system (BEL JAPAN, INC., Osaka, Japan). In this analysis, 0.050 g of the calcined was outgassed at 220 °C for 2 h in argon (Ar) flow of 30 mL min^{-1}, followed by cooling to ambient temperatures. Consequently, the catalyst sample was reduced in the temperature programmed from 40 to 850 °C under 5 vol.% H_2/Ar flow of 30 mL min^{-1}. The H_2 uptake was monitored by thermal conductivity detector (TCD).

The basicity of the reduced catalysts was evaluated by temperature-programmed desorption of carbon dioxide (CO_2-TPD) on the similar instrument of the H_2-TPR. Prior the measurement, 0.050 g of catalyst sample was pre-treated by heating at 220 °C under He (30 mL/min) for 2 h, following by cooling 40 °C. Next, the catalyst was *in-situ* reduced at 600 °C for 2 h with pure H_2 flow of 30 mL min^{-1} and cooled to 40 °C in flowing He. Then, a pure CO_2 gas was introduced to be adsorbed on the catalyst surface at 40 °C for 1.5 h. Afterward, the catalyst was purged in He flow to flush physically adsorbed CO_2 on the surface. After purging, the catalyst was heated from 50 to 700 °C at a rate of 10 °C min^{-1} in He flow, and the desorbed CO_2 was monitored by TCD.

The quantity and types of the carbon deposition on the spent catalysts during the dry methane reforming reaction were estimated by the thermogravimetric analysis (TGA) using a METTLER TOLEDO thermogravimetric analyzer (METTLER TOLEDO, Columbus, OH, USA)

The CRM reaction was demonstrated in a tubular fixed-bed reactor at 600 °C for 6 h. Prior to the reaction, 0.200 g of catalyst was in-situ reduced at 600 °C for 3 h in a H_2 atmosphere (30 mL min^{-1}). Then, the feed molar composition of CH_4:CO_2:N_2 = 4:2.5:2 at an overall flow rate of 85 mL min^{-1} was introduced to the reactor. Afterwards, the exit gases were analyzed by an on-line gas chromatography (Agilent GC7890A Agilent, Santa Clara, CA, USA) equipped with a TCD detector. The catalyst performance was elucidated in terms of a CH_4 conversion (Eq. (5)), CO_2 conversion (Eq. (6)) and H_2/CO ratio (Eq. (7)) as expressed in the following equations:

$$\%CH_4 \text{ conversion} = \frac{\text{Flow rate of } CH_{4,in} - \text{Flow rate of } CH_{4,out}}{\text{Flow rate of } CH_{4,in}} \times 100 \quad (5)$$

$$\%CO_2 \text{ conversion} = \frac{\text{Flow rate of } CO_{2,in} - \text{Flow rate of } CO_{2,out}}{\text{Flow rate of } CO_{2,in}} \times 100 \quad (6)$$

$$H_2/CO \text{ ratio} = \frac{\text{Flow rate of } H_{2,out}}{\text{Flow rate of } CO_{out}} \quad (7)$$

Results and discussion

Characterization

The X-ray diffractograms of the Al_2O_3 support and all catalyst samples calcined at 650 °C are presented in **Figure 1**. The broad diffraction peaks of amorphous γ-Al_2O_3 phase at 2-theta of 38, 45 and 67 ° (JCPDS No. 29-0063) were observed in the diffractograms of all samples. Peaks corresponding to the Co_3O_4 phase at 19, 37, 43 and 65 ° were detectable in diffractogram of 7Co-3ZrO_2/Al_2O_3, 9Co-1ZrO_2/Al_2O_3 and 4.5Ni-4.5Co-1ZrO_2/Al_2O_3 catalysts. In the 9Ni-1ZrO_2/Al_2O_3 catalyst, the discrete peaks of NiO phase located at 37, 43 and 66 ° were discovered [17]. The characteristic diffractograms at 2-theta of 19, 37, 43 and 66 ° can be attributed to the non-completely single-phase structure of the $CoAl_2O_4$ (or $NiAl_2O_4$) spinel due to the certain Co^{2+} (or Ni^{2+}) ions substituted into the γ-Al_2O_3 lattice during catalyst preparation [18]. It should be noted that diffraction peaks of ZrO_2 cannot be detected due to its low content.

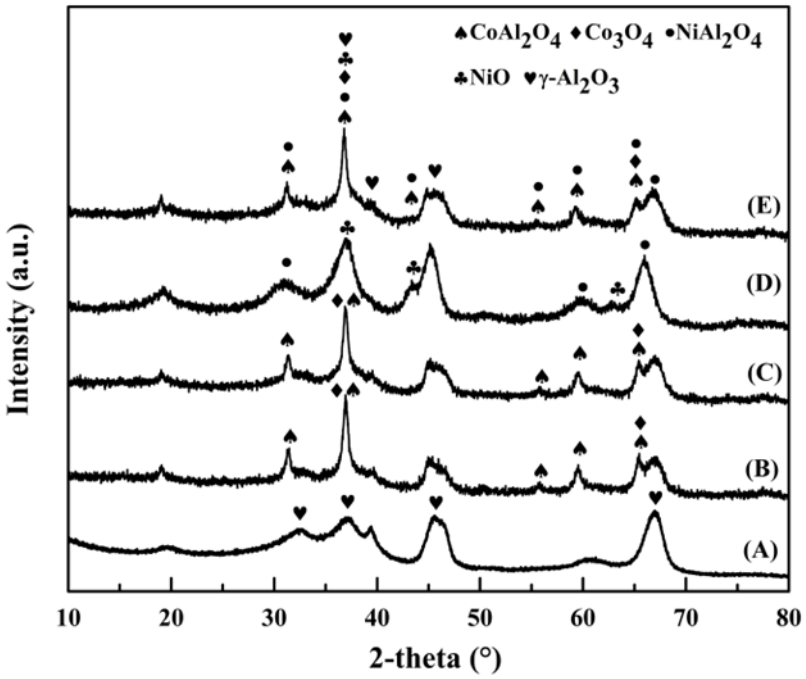

Figure 1 The X-ray diffraction pattern of all sample (A) γ-Al_2O_3, (B) 7Co-3ZrO_2/Al_2O_3, (C) 9Co-1ZrO_2/Al_2O_3, (D) 9Ni-1ZrO_2/Al_2O_3 and (E) 4.5Ni-4.5Co-1ZrO_2/Al_2O_3.

The N_2 adsorption-desorption isotherm and pore size distribution of Al_2O_3 support as well as all calcined catalysts are depicted in **Figures 2(A)** - **2(B)**, respectively. The physisorption isotherm of all samples are a type IV isotherm with an H2-shaped hysteresis loop, associating to the cylindrical-shaped channels with the non-uniform pores [19] (**Figure 2(A)**). When the Co (and/or Ni) and ZrO_2 were impregnated onto Al_2O_3 support, the hysteresis loops of all catalysts imply a lower pore volume than the Al_2O_3 support at the relative pressure (P/P_0) of 0.60 - 0.95 because of the pore blockage during the impregnation [20]. The pore size distribution curves (**Figure 2(B)**) were elucidated by the Barret-Joyner-Halenda (BJH) method and the average pore size results were computed from the distribution (**Table 1**). The Al_2O_3 support has the broad pore size distribution averaged at 6.7 nm with the surface area of 160.7 $m^2\,g^{-1}$. After Co (and/or Ni) and ZrO_2 loading, 7Co-1ZrO_2/Al_2O_3, 9Co-1ZrO_2/Al_2O_3, 9Ni-1ZrO_2/Al_2O_3 and 4.5Ni-4.5-1ZrO_2/Al_2O_3 catalysts show a narrow average pore size peak centered about 4.0 - 4.6 nm and the lower surface area (about 133.0 - 143.4 $m^2\,g^{-1}$). These results can be attributed to the blocking phenomenon of mesoporous Al_2O_3 by Co_2O_3 or/and NiO with ZrO_2 particles.

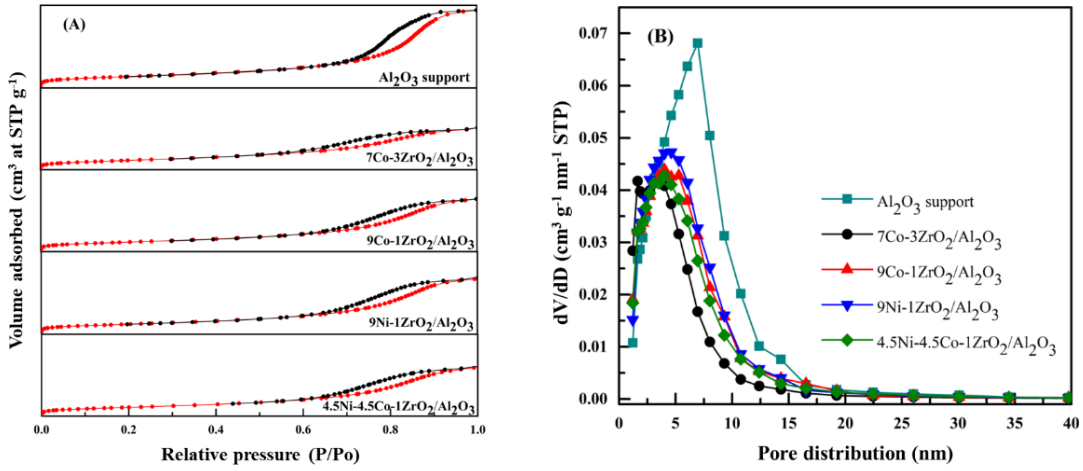

Figure 2 (A) N_2 adsorption-desorption isotherms and (B) BJH pore size distributions of γ-Al_2O_3, 7Co-3ZrO_2/Al_2O_3, 9Co-1ZrO_2/Al_2O_3, 9Ni-1ZrO_2/Al_2O_3 and 4.5Ni-4.5Co-1ZrO_2/Al_2O_3.

Table 1 Textural properties of all samples.

Samples	N_2 adsorption-desorption		
	Surface area ($m^2 g^{-1}$)	**Total pore volume ($cm^3 g^{-1}$)**	**Average pore size (nm)**
Al_2O_3 support	160.7	0.51	6.7
7Co-3ZrO_2/Al_2O_3	143.4	0.27	4.6
9Co-1ZrO_2/Al_2O_3	141.9	0.34	4.0
9Ni-1ZrO_2/Al_2O_3	140.0	0.36	4.0
4.5Ni-4.5Co-1ZrO_2/Al_2O_3	133.0	0.32	4.6

The reducibility property corresponds to oxide species and the interaction of oxide components. Reduction of calcined catalyst samples (**Figure 3**) were investigated in the temperature range of 50 to 700 °C using H_2-TPR. Peaks around 150 - 400 °C are referred to the reaction of oxide species (Co_3O_4 or/and NiO) that interact weakly with Al_2O_3 support. Peaks appearing in 400 - 580 °C are corelated to the reduction of CoO to Co species (for 7Co-3ZrO_2/Al_2O_3 and 9Co-1ZrO_2/Al_2O_3) and the reduction of NiO having a moderate interaction with Al_2O_3 support (for 9Ni-1ZrO_2/Al_2O_3). Third reduction peak at temperature over 580 °C is ascribed to the reduction of the Co^{2+} and Ni^{2+} species in the strong metal-support interaction (SMSI) oxides such as $CoAl_2O_4$ and $NiAl_2O_4$ spinel phase, respectively [21-23]. The H_2-TPR profile of 9Co-1ZrO_2/Al_2O_3 catalyst shows the peak shoulder centered at 425 °C, the reduction peak centered at 525 °C, and the peak shoulder centered at 635 °C. The results are evident in the reduction of the $Co_3O_4 \rightarrow$ CoO → Co species in the moderate associated strong interaction with Al_2O_3 support [24,25]. When 7 %wt. Co and 3 %wt.ZrO_2 were impregnated onto Al_2O_3 support, H_2-TPR peaks of 7Co-3ZrO_2/Al_2O_3 shift slightly toward lower temperatures (centered about 400, 510 and 625 °C) and the area undercurve is larger. It indicates that adding ZrO_2 content up to 3 %wt results in more Co on the surface due to weaker metal-support interaction compared to 9Co-1ZrO_2/Al_2O_3 [26]. The area under reduction curves of 4.5Ni-4.5Co-1ZrO_2/Al_2O_3 and 9Ni-1ZrO_2/Al_2O_3 catalysts are dramatically lower than 7Co-3ZrO_2/Al_2O_3 and 9Co-1ZrO_2/Al_2O_3 catalysts, especially 9Ni-1ZrO_2/Al_2O_3. The TPR profile of 4.5Ni-4.5Co-1ZrO_2/Al_2O_3 shows peak centered at 400 °C and the higher temperature peak centered at 600 °C. The peak at medium temperature range relates to simultaneously the reduction of Co_3O_4 to CoO, CoO to Co and NiO to Ni. The peak at high temperature range corresponds to the reduction CoO and NiO incorporated to Al_2O_3 support ($CoAl_2O_4$ and $NiAl_2O_4$ spinel structure). The reduction curve of 9Ni-1ZrO_2/Al_2O_3 with board peaks starting at 500 °C reflecting the reduction of nickel oxide species in NiO-Al_2O_3 support accompanies with $NiAl_2O_4$ species interaction. These results occur because Co can be inherently incorporated with ZrO_2 [27]. Thus, Co in Co-ZrO_2 has less interaction with Al_2O_3 compared to Ni in Ni-ZrO_2.

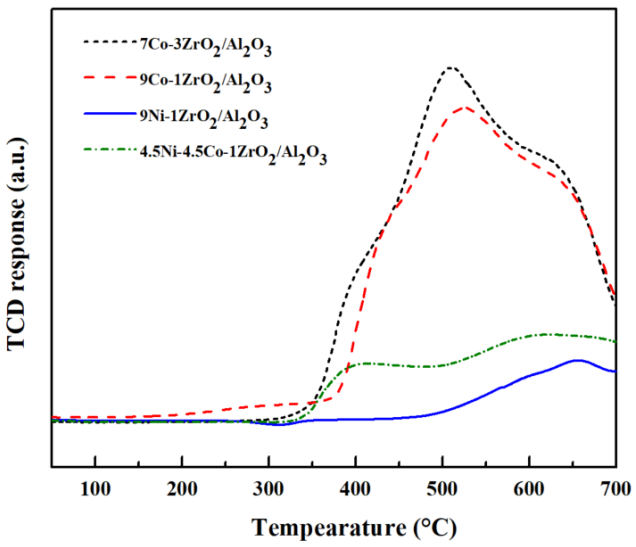

Figure 3 H_2-TPR profile of all catalyst samples.

The CO_2 adsorption ability according to the distribution of basic sites on the reduced catalyst surface was evaluated via CO_2-TPD measurement. The desorption peaks in CO_2-TPD profiles (**Figure 4)** indicate 3 types of basic site strength depending on the desorption temperature. The desorption of CO_2 at the relative low temperature (50 - 150 °C (or 200 °C)) from weak basic sites are associated to the adsorption of CO_2 over the surface hydroxyl groups. The desorption of CO_2 at the relative medium temperature (150 (or 200 - 450 °C) from moderate basic sites are corresponded to the adsorption of CO_2 over the Lewis acid-base pairing. The desorption of CO_2 at the relative high temperature (> 450 °C) from strong basic sites are connected to the adsorption of CO_2 over the low-coordination surface oxygen anions [27-30]. The amount of CO_2 desorption determined from the profiles are reported in **Table 2**. Compared to all present catalysts, 7Co-3ZrO_2/Al_2O_3 provides the highest number of weak basic sites and 4.5Ni-4.5Co-1ZrO_2/Al_2O_3 has the second highest number of weak basic sites than other catalysts. 9Co-1ZrO_2/Al_2O_3 catalyst presented highest amount of moderate basic sites. The smallest number of basic sites were found on 9Ni-1ZrO_2/Al_2O_3. It can be explained that oxygen vacancy sites near Co in ZrO_2 effectively absorb and dissociate CO_2 [27].

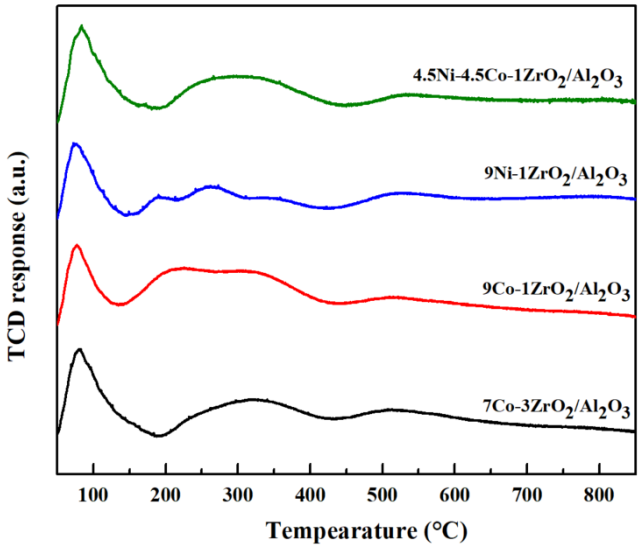

Figure 4 CO_2-TPD profile of all reduced catalyst samples.

Table 2 Deconvolution of the CO_2-TPD profiles for all reduced catalysts.

Samples	CO_2-TPD deconvolution (mmol g^{-1})			
	Weak	Moderate	Strong	Total basicity
7Co-3ZrO_2/Al_2O_3	0.088	0.055	0.050	0.193
9Co-1ZrO_2/Al_2O_3	0.049	0.091	0.048	0.188
9Ni-1ZrO_2/Al_2O_3	0.060	0.046	0.045	0.151
4.5Ni-4.5Co-1ZrO_2/Al_2O_3	0.078	0.070	0.088	0.236

Catalytic activity, selectivity and stability

The CRM test in the case that CO_2 is the limiting reagent was performed on the present catalysts at 600 °C for 6 h and the results are reported in **Figures 5(A) - 5(C)**. The order of CO_2 conversion, CH_4 conversion and H_2/CO ratio was found in the similar trend as 9Co-1ZrO_2/Al_2O_3 > 7Co-3ZrO_2/Al_2O_3 > 9Ni-1ZrO_2/Al_2O_3 > 4.5Ni-4.5Co-1ZrO_2/Al_2O_3 catalysts. In this case, Co-based catalysts show the highest activity (**Figures 5(A) - 5(B)**) which the excellent selectivity toward H_2 (**Figure 5(C)**).

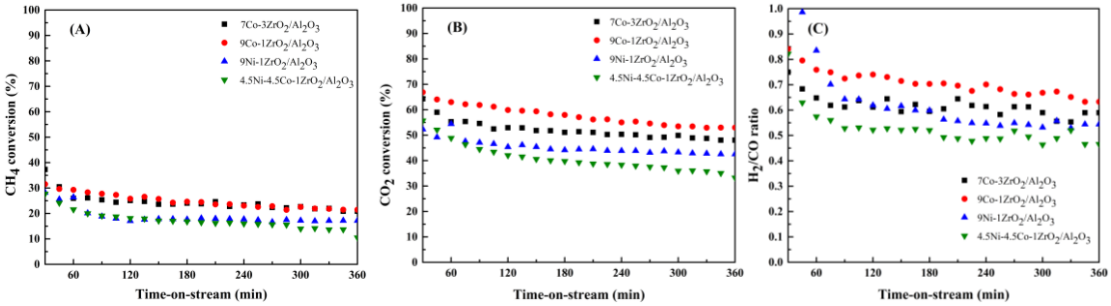

Figure 5 (A) CH_4 conversion, (B) CO_2 conversion and, (C) H_2/CO ratio for carbon dioxide reforming of methane (CRM) of all catalysts: Reaction conditions 600 °C and 1 atm for 6 h.

The anti-coking ability of the present catalysts in the CRM were evaluated via TGA measurement (**Figure 6** and **Table 3**). Quantity of carbon deposition can be determined by the value of weight loss and types of coke are evaluated from the temperature ranges of weight loss during TGA measurement. Amorphous carbon, graphitic carbon and whisker carbon are oxidized at low (150 - 300 °C), medium (300 - 550 °C) and high temperatures (> 550 °C), respectively [31]. The spent 9Ni-1ZrO_2/Al_2O_3 shows the maximum coke accumulation with almost only the whisker carbon, the hardest type for removal [32]. The second maximum coke accumulation was observed on the spent 9Co-1ZrO_2/Al_2O_3 containing all 3 types of carbon deposition. Among all spent catalysts, the spent 4.5Ni-4.5Co-1ZrO_2/Al_2O_3 and spent 7Co-3ZrO_2/Al_2O_3 with 2 types of carbon deposition (Filamentous carbon was rarely detected) show small amount of carbon deposition. The spent 7Co-3ZrO_2/Al_2O_3 that also presents high activities has the minimum coke deposit.

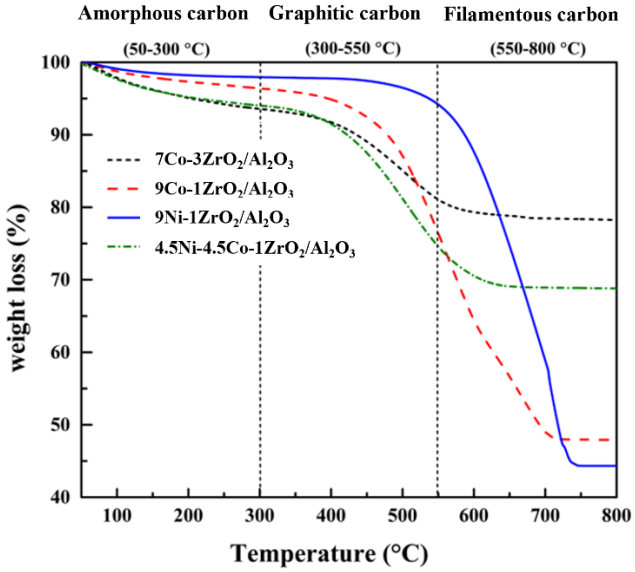

Figure 6 TGA profiles of all spent catalysts.

Table 3 Weight loss per gram of all spent catalysts.

Spent catalysts	Weight loss per gram (mg g^{-1})
7Co-3ZrO_2/Al_2O_3	173
9Co-1ZrO_2/Al_2O_3	345
9Ni-1ZrO_2/Al_2O_3	367
4.5Ni-4.5Co-1ZrO_2/Al_2O_3	245

CRM reaction is known to consist of CH_4 adsorption-dissociation mechanism creating C^* and H^* (*denotes an adsorption state) and CO_2 adsorption-dissociation mechanism creating CO^* and O^*. If C^* can be oxidized effectively, less amount of coke will be formed and easily eliminated. Considering the feed composition and the inherent of reactants, the concentration of CO_2 in the feed is less than that of CH_4 and the chemical bond in CO_2 is very strong due to the stable bond energy of the CO_2 molecule [33]. Ni-based catalysts are normally active toward CH_4 and less active for CO_2 [6]. Thus, 9Ni-1ZrO_2/Al_2O_3 shows low activity with large amount of coke for CRM at low CO_2 as it hardly drives CO_2 adsorption-dissociation mechanism. The effective CRM performance of Co-ZrO_2/Al_2O_3 for low CO_2 condition is indeed a consequence of the oxophilicity of Co ($Co_2O_3 \rightarrow CoO \rightarrow Co$) accompanied with oxygen vacancy sites near Co in ZrO_2 [27]. As the high activity for the limiting reagent (CO_2), the catalysts then provide high conversion of the excess reactant (CH_4). When the Co-based catalysts have high moderate base sites, it provides high oxophilic properties. Consequently, 9Co-1ZrO_2/Al_2O_3 shows higher activity than 7Co-3ZrO_2/Al_2O_3. When the ratio of ZrO_2 to Co is greater, the number of oxygen vacancy sites are generated resulting in moving more O^* atoms through the active surface [34-36]. Atom of O^* can directly oxidized C^* or produce the surface hydroxyl (-OH^*, related to CO_2-TPD result). Then, surface carbon of 7Co-3ZrO_2/Al_2O_3 catalysts is effectively oxidized by O^* and OH^*. This property of 7Co-3ZrO_2/Al_2O_3, however, decreased the selectivity toward H_2 compared to 9Co-1ZrO_2/Al_2O_3 catalyst. Similarly, 4.5Ni-4.5Co-1ZrO_2/Al_2O_3 catalyst also shows the ability to oxidize coke but provides lowest activity among all for this reaction condition. It can be explained by Ni-Co alloy formation after the reduction that subtract nature activity of Co.

Conclusions

The Co-ZrO_2/Al_2O_3 developed in this work illustrates the great CRM performance when CO_2 is the limiting reagent. Co with ZrO_2 promoter provides oxophilicity accompanied with active sites toward CO_2 as well as the oxygen transfer. Therefore, Co-ZrO_2/Al_2O_3 catalysts present an appropriate activity on CRM operated at severe condition. 9%wtCo-1%wtZrO_2/Al_2O_3 catalyst provides high activity with selective toward H_2. The superior of coke prevention was observed on 7%wtCo-3%wtZrO_2/Al_2O_3 even when CH_4 is an excess reagent. Thus, this work reveals that Co-ZrO_2/Al_2O_3 catalysts can be considered as the candidate catalyst to develop for CRM process in petroleum industry.

Acknowledgements

The authors gratefully acknowledge the financial and infrastructure support of Thailand Institute of Nuclear Technology, Thailand (Public Organization) (TINT) through TINT to university program.

References

[1] D Reay and P Smith. *Methane and climate change*. Routledge, London, 2010.
[2] AM Ranjekar and GD Yadav. Dry reforming of methane for syngas production: A review and assessment of catalyst development and efficacy. *J. Indian Chem. Soc.* 2021; **98**, 100002.
[3] DA Wood, C Nwaoha and BF Towler. Gas-to-liquids (GTL): A review of an industry offering several routes for monetizing natural gas. *J. Nat. Gas Sci. Eng.* 2012; **9**, 196-208.
[4] V Ribun, S Boichenko and U Kale. Advances in gas-to-liquid technology for environmentally friendly fuel synthesis: Analytical review of world achievements. *Energ. Rep.* 2023; **9**, 5500-8.
[5] F Galli, JJ Lai, JD Tommaso, G Pauletto and GS Patience. Gas to liquids techno-economics of associated natural gas, bio gas, and landfill gas. *Processes* 2021; **9**, 1568.
[6] N Dharmasaroja, T Ratana, S Tungkamani, T Sornchamni, DS Simakov and M Phongaksorn. The effects of CeO_2 and Co doping on the properties and the performance of the Ni/Al_2O_3-MgO catalyst for the combined steam and CO_2 reforming of methane using ultra-low steam to carbon ratio. *Catalysts* 2020; **10**, 1450.
[7] W Sumarasingha, S Supasitmongkol and M Phongaksorn. The effect of ZrO_2 as different components of Ni-based catalysts for CO_2 reforming of methane and combined steam and CO_2 reforming of methane on catalytic performance with coke formation. *Catalysts* 2021; **11**, 984.
[8] H Deng and Y Guo. Artificial neural network model for the prediction of methane bi-reforming products using CO_2 and steam. *Processes* 2022; **10**, 1052.
[9] HS Whang, J Lim, MS Choi, J Lee and H Lee. Heterogeneous catalysts for catalytic CO_2 conversion into value-added chemicals. *BMC Chem. Eng.* 2019; **1**, 9.

[10] BJ Kim, HR Park, YL Lee, SY Ahn, KJ Kim, GR Hong and HS Roh. Customized Ni-MgO-ZrO_2 catalysts for the dry reforming of methane using coke oven gas: Optimizing the MgO content. *J. CO2 Utilization* 2023; **68**, 102379.
[11] AF Cunha, S Morales-Torres, LM Pastrana-Martínez, AA Martins, TM Mata, NS Caetano and JM Loureiro. Syngas production by bi-reforming methane on an Ni-K-promoted catalyst using hydrotalcites and filamentous carbon as a support material. *RSC Adv.* 2020; **10**, 21158-73
[12] J Han, Y Zhan, J Street, F To and F Yu. Natural gas reforming of carbon dioxide for syngas over Ni-Ce-Al catalysts. *Int. J. Hydrogen Energ.* 2017; **42**, 18364-74.
[13] R Dębek, M Motak, ME Galvez, T Grzybek and PD Costa. Promotion effect of zirconia on Mg(Ni,Al)O mixed oxides derived from hydrotalcites in CO_2 methane reforming. *Appl. Catal. B Environ.* 2018; **223**, 36-46.
[14] C Zhang, X Geng, X Zhang, Y Gnanou and X Feng. Alkyl borane-mediated metal-free ring-opening (co)polymerizations of oxygenated monomers. *Progr. Polymer Sci.* 2022; **136**, 101644.
[15] Y Lou, M Steib, Q Zhang, K Tiefenbacher, A Horváth, A Jentys and JA Lercher. Design of stable Ni/ZrO_2 catalysts for dry reforming of methane. *J. Catal.* 2017; **356**, 147-56.
[16] Z Bian, S Das, MH Wai, P Hongmanorom and S Kawi. A review on bimetallic nickel-based catalysts for CO_2 reforming of methane. *Chem. Eur.* 2017; **18**, 3117-34.
[17] M Cai, J Wen, W Chu, X Cheng and Z Li. Methanation of carbon dioxide on Ni/ZrO_2-Al_2O_3 catalysts: Effects of ZrO_2 promoter and preparation method of novel ZrO_2-Al_2O_3 carrier. *J. Nat. Gas Chem.* 2011; **20**, 318-24.
[18] A Iriondo, VL Barrio, JF Cambra, PL Arias, MB Guemez, MC Sanchez-Sanchez, RM Navarro and JLG Fierro. Glycerol steam reforming over Ni catalysts supported on ceria and ceria-promoted alumina. *Int. J. Hydrogen Energ.* 2010; **35**, 11622-33.
[19] Z Wang, X Jiang, M Pan and Y Shi. Nano-scale pore structure and its multi-fractal characteristics of tight sandstone by N_2 adsorption/desorption analyses: A case study of Shihezi formation from the Sulige gas filed, Ordos Basin, China. *Minerals* 2020; **10**, 377.
[20] W Liu, Y Zhang, S Wang, L Bai, Y Deng and J Tao. Effect of pore size distribution and amination on adsorption capacities of polymeric adsorbents. *Molecules* 2021; **26**, 5267.
[21] M Zhumabek, G Xanthopoulou, SA Tungatarova, TS Baizhumanova, G Vekinis and YD Murzin. Biogas reforming over Al-Co catalyst prepared by solution combustion synthesis method. *Catalysts* 2021; **11**, 274.
[22] R Wang, Y Li, R Shi and M Yang. Effect of metal - support interaction on the catalytic performance of Ni/Al_2O_3 for selective hydrogenation of isoprene. *J. Mol. Catal. Chem.* 2011; **344**, 122-7.
[23] AW Budiman, SH Song, TS Chang, CH Shin and MJ Choi. Dry reforming of methane over cobalt catalysts: A literature review of catalyst development. *Catal. Surv. Asia* 2012; **16**, 183-97.
[24] Z Liu, J Li, M Buettner, R Ranganathan, M Uddi and R Wang. Metal - support Interactions in CeO_2 and SiO_2 supported cobalt catalysts: Effect of support morphology, reducibility and interfacial configuration. *ACS Appl. Mater. Interfac.* 2019; **11**, 17035-49.
[25] I Luisetto, S Tuti and ED Bartolomeo. Co and Ni supported on CeO_2 as selective bimetallic catalyst for dry reforming of methane. *Int. J. Hydrogen Energ.* 2012; **37**, 15992-9.
[26] H Wu, Y Yang, H Suo, M Qing, L Yan, B Wu and Y Li. Effects of ZrO_2 promoter on physic-chemical properties and activity of Co/TiO_2-SiO_2 Fischer-Tropsch catalysts. *J. Mol. Catal. Chem.* 2015; **396**, 108-19.
[27] NHM Dostagir, R Rattanawan, M Gao, J Ota, JY Hasegawa, K Asakura and A Shrotri. Co single atoms in ZrO_2 with inherent oxygen vacancies for selective hydrogenation of CO_2 to CO. *ACS Catal.* 2021; **11**, 9450-61.
[28] M Dan, M Mihet, G Borodi and MD Lazar. Combined steam and dry reforming of methane for syngas production from biogas using bimodal pore catalysts. *Catal. Today* 2021; **366**, 87-96.
[29] PH Phuong, LC Loc, N Tri, NP Anh and HC Anh. Effect of NH_3 alkalization and MgO promotion on the performance of Ni/SBA-15 catalyst in combined steam and carbon dioxide reforming of methane. *J. Nanomaterials* 2021; **2021**, 5570866.
[30] U Sikander, S Sufian and MA Salam. A review of hydrotalcite based catalysts for hydrogen production systems. *Int. J. Hydrogen Energ.* 2017; **42**, 19851-68.
[31] A Ochoa, J Bilbao, AG Gayubo and P Castaño. Coke formation and deactivation during catalytic reforming of biomass and waste pyrolysis products: A review. *Renew. Sustain. Energ. Rev.* 2020; **119**, 109600.

[32] D Yao, H Yang, H Chen and PT Williams. Co-precipitation, impregnation and sol-gel preparation of Ni catalysts for pyrolysis-catalytic steam reforming of waste plastics. *Appl. Catal. B Environ.* 2018; **239**, 565-77.

[33] AF Cunha, TM Mata, NS Caetano, AA Martins and JM Loureiro. Catalytic bi-reforming of methane for carbon dioxide ennoblement. *Energ. Rep.* 2020; **6**, 74-9.

[34] M Zhang, J Zhang, Y Wu, J Pan, Q Zhang, Y Tan and Y Han. Insight into the effects of the oxygen species over Ni/ZrO_2 catalyst surface on methane reforming with carbon dioxide. *Appl. Catal. B Environ.* 2019; **244**, 427-37.

[35] AH Fakeeha, Y Arafat, AA Ibrahim, H Shaikh, H Atia, AE Abasaeed and AS Al-Fatesh. Highly selective syngas/H_2 production via partial oxidation of CH_4 using (Ni, Co and Ni-Co)/ZrO_2-Al_2O_3 catalysts: Influence of calcination temperature. *Processes* 2019; **7**, 141.

[36] W Liu, L Li, X Zhang, Z Wang, X Wang and H Peng. Design of Ni-ZrO_2@ SiO_2 catalyst with ultra-high sintering and coking resistance for dry reforming of methane to prepare syngas. *J. CO2 Utilization* 2018; **27**, 297-307.